

Broadband amplification by picosecond OPCPA in DKDP pumped at 515 nm

Christoph Skrobol,^{1,2,4,*} Izhar Ahmad,^{1,3,4,5} Sandro Klingebiel,¹ Christoph Wandt,¹
Sergei A. Trushin,¹ Zsuzsanna Major,^{1,2} Ferenc Krausz,^{1,2} and Stefan Karsch^{1,2}

¹Max-Planck-Institut für Quantenoptik, Hans-Kopfermann-Str. 1 D-85748 Garching, Germany

²Department für Physik, Ludwig-Maximilians-Universität München, Am Coulombwall 1 D-85748 Garching, Germany

³Optics Laboratories, P.O. 1021, Nilore, Islamabad, Pakistan

⁴These authors contributed equally to this work

⁵izhar916@yahoo.com

*christoph.skrobol@mpq.mpg.de

Abstract: On the quest towards reaching petawatt-scale peak power light pulses with few-cycle duration, optical parametric chirped pulse amplification (OPCPA) pumped on a time scale of a few picoseconds represents a very promising route. Here we present an experimental demonstration of few-ps OPCPA in DKDP, in order to experimentally verify the feasibility of the scheme. Broadband amplification was observed in the wavelength range of 830-1310 nm. The amplified spectrum supports two optical cycle pulses, at a central wavelength of ~920 nm, with a pulse duration of 6.1 fs (FWHM). The comparison of the experimental results with our numerical calculations of the OPCPA process showed good agreement. These findings confirm the reliability of our theoretical modelling, in particular with respect to the design for further amplification stages, scaling the output peak powers to the petawatt scale.

©2012 Optical Society of America

OCIS codes: (190.4970) Parametric oscillators and amplifiers; (190.4975) Parametric processes; (190.4410) Nonlinear optics, parametric processes; (190.4223) Nonlinear wave mixing.

References and links

1. J. Faure, Y. Glinec, A. Pukhov, S. Kiselev, S. Gordienko, E. Lefebvre, J. P. Rousseau, F. Burgy, and V. A. Malka, "A laser-plasma accelerator producing monoenergetic electron beams," *Nature* **431**(7008), 541–544 (2004).
2. S. P. D. Mangles, C. D. Murphy, Z. Najmudin, A. G. R. Thomas, J. L. Collier, A. E. Dangor, E. J. Divall, P. S. Foster, J. G. Gallacher, C. J. Hooker, D. A. Jaroszynski, A. J. Langley, W. B. Mori, P. A. Norreys, F. S. Tsung, R. Viskup, B. R. Walton, and K. Krushelnick, "Monoenergetic beams of relativistic electrons from intense laser-plasma interactions," *Nature* **431**(7008), 535–538 (2004).
3. C. G. R. Geddes, C. S. Toth, J. Van Tilborg, E. Esarey, C. B. Schroeder, D. Bruhwiler, C. Nieter, J. Cary, and W. P. Leemans, "High-quality electron beams from a laser wakefield accelerator using plasma-channel guiding," *Nature* **431**(7008), 538–541 (2004).
4. M. Geissler, J. Schreiber, and J. Meyer-ter-Vehn, "Bubble acceleration of electrons with few-cycle laser pulses," *New J. Phys.* **8**(9), 186 (2006).
5. Y. Nomura, R. Hörlein, P. Tzallas, B. Dromey, S. Rykovanov, Zs. Major, J. Osterhoff, S. Karsch, L. Veisz, M. Zepf, D. Charalambidis, F. Krausz, and G. D. Tsakiris, "Attosecond phase locking of harmonics emitted from laser-produced plasmas," *Nat. Phys.* **5**(2), 124–128 (2009).
6. D. Strickland and G. Mourou, "Compression of amplified chirped optical pulses," *Opt. Commun.* **56**(3), 219–221 (1985).
7. A. Dubietis, G. Jonušauskas, and A. Piskarskas, "Powerful femtosecond pulse generation by chirped and stretched pulse parametric amplification in BBO crystal," *Opt. Commun.* **88**(4-6), 437–440 (1992).
8. V. V. Lozhkarev, G. I. Freidman, V. N. Ginzburg, E. V. Katin, E. A. Khazanov, A. V. Kirsanov, G. A. Luchinin, A. N. Mal'shakov, M. A. Martyanov, O. V. Palashov, A. K. Poteomkin, A. M. Sergeev, A. A. Shaykin, and I. V. Yakovlev, "Compact 0.56 petawatt laser system based on optical parametric chirped pulse amplification in KD*P crystals," *Laser Phys. Lett.* **4**(6), 421–427 (2007).

9. O. Chekhlov, E. J. Divall, K. Ertel, S. J. Hawkes, C. J. Hooker, I. N. Ross, P. Matousek, C. Hernandez-Gomez, I. Musgrave, Y. Tang, T. Winstone, D. Neely, R. Clarke, P. Foster, S. J. Hancock, B. E. Wyborn, and J. L. Collier, "Development of petawatt laser amplification systems at the Central Laser Facility," *Proc. SPIE* **6735**, 67350J (2007).
10. S. Adachi, N. Ishii, T. Kanai, A. Kosuge, J. Itatani, Y. Kobayashi, D. Yoshitomi, K. Torizuka, and S. Watanabe, "5-fs, Multi-mJ, CEP-locked parametric chirped-pulse amplifier pumped by a 450-nm source at 1 kHz," *Opt. Express* **16**(19), 14341–14352 (2008).
11. D. Herrmann, L. Veisz, R. Tautz, F. Tavella, K. Schmid, V. Pervak, and F. Krausz, "Generation of sub-three-cycle, 16 TW light pulses by using noncollinear optical parametric chirped-pulse amplification," *Opt. Lett.* **34**(16), 2459–2461 (2009).
12. X. Gu, G. Marcus, Y. Deng, T. Metzger, C. Teisset, N. Ishii, T. Fuji, A. Baltuska, R. Butkus, V. Pervak, H. Ishizuki, T. Taira, T. Kobayashi, R. Kienberger, and F. Krausz, "Generation of carrier-envelope-phase-stable 2-cycle 740- μ J pulses at 2.1- μ m carrier wavelength," *Opt. Express* **17**(1), 62–69 (2009).
13. D. Brida, C. Manzoni, G. Cirimi, M. Marangoni, S. Bonora, P. Villaresi, S. De Silvestri, and G. Cerullo, "Few-optical-cycle pulses tunable from the visible to the mid-infrared by optical parametric amplifiers," *J. Opt.* **12**(1), 013001 (2010).
14. G. Cerullo and S. De Silvestri, "Ultrafast optical parametric amplifiers," *Rev. Sci. Instrum.* **74**(1), 1–18 (2003).
15. N. Ishii, L. Turi, V. S. Yakovlev, T. Fuji, F. Krausz, A. Baltuska, R. Butkus, G. Veitas, V. Smilgevičius, R. Danielius, and A. Piskarskas, "Multimillijoule chirped parametric amplification of few-cycle pulses," *Opt. Lett.* **30**(5), 567–569 (2005).
16. S. Witte, R. T. Zinkstok, A. L. Wolf, W. Hogervorst, W. Ubachs, and K. S. E. Eikema, "A source of 2 terawatt, 2.7 cycle laser pulses based on noncollinear optical parametric chirped pulse amplification," *Opt. Express* **14**(18), 8168–8177 (2006).
17. O. Chalus, P. K. Bates, M. Smolarski, and J. Biegert, "Mid-IR short-pulse OPCPA with micro-Joule energy at 100kHz," *Opt. Express* **17**(5), 3587–3594 (2009).
18. K. W. Aniolek, R. L. Schmitt, T. J. Kulp, B. A. Richman, S. E. Bisson, and P. E. Powers, "Microlaser-pumped periodically poled lithium niobate optical parametric generator-optical parametric amplifier," *Opt. Lett.* **25**(8), 557–559 (2000).
19. B. Zhao, Y. Jiang, K. Sueda, N. Miyana, and T. Kobayashi, "Ultrabroadband noncollinear optical parametric amplification with LBO crystal," *Opt. Express* **16**(23), 18863–18868 (2008).
20. V. V. Lozhkarev, G. I. Freidman, V. N. Ginzburg, E. A. Khazanov, O. V. Palashov, A. M. Sergeev, and I. V. Yakovlev, "Study of broadband optical parametric chirped pulse amplification in a DKDP crystal pumped by the second harmonic of a Nd:YLF laser," *Laser Phys.* **15**, 1319–1333 (2005).
21. Y. Mori, I. Kuroda, S. Nakajima, T. Sasaki, and S. Nakai, "New nonlinear optical crystal: cesium lithium borate," *Appl. Phys. Lett.* **67**(13), 1818–1820 (1995).
22. B. Zhao, X. Liang, Y. Leng, Y. Jiang, C. Wang, H. Lu, J. Du, Z. Xu, and D. Shen, "Degenerated optical parametric chirped-pulse amplification with cesium lithium borate," *Appl. Opt.* **45**(3), 565–568 (2006).
23. E. A. Khazanov and A. M. Sergeev, "Petawatt lasers based on optical parametric amplifiers: their state and prospects," *Phys. Usp.* **51**, 969–974 (2008).
24. S. Karsch, Zs. Major, J. Fülöp, I. Ahmad, T. Wang, A. Henig, S. Kruber, R. Weingartner, M. Siebold, J. Hein, C. Wandt, S. Klingebiel, J. Osterhoff, R. Hörlein, and F. Krausz, "The Petawatt Field Synthesizer: a new approach to ultrahigh field generation," in *Advanced Solid-State Photonics*, OSA Technical Digest Series (CD) (Optical Society of America, 2008), paper WF1.
25. Zs. Major, S. A. Trushin, I. Ahmad, M. Siebold, C. Wandt, S. Klingebiel, T.-J. Wang, J. A. Fülöp, A. Henig, S. Kruber, R. Weingartner, A. Popp, J. Osterhoff, R. Hörlein, J. Hein, V. Pervak, A. Apolonski, F. Krausz, and S. Karsch, "Basic concepts and current status of the Petawatt Field Synthesizer — a new approach to ultrahigh field generation," *Rev. Laser Eng.* **37**, 431–436 (2009).
26. C. Wandt, S. Klingebiel, M. Siebold, Z. Major, J. Hein, F. Krausz, and S. Karsch, "Generation of 220 mJ nanosecond pulses at a 10 Hz repetition rate with excellent beam quality in a diode-pumped Yb:YAG MOPA system," *Opt. Lett.* **33**(10), 1111–1113 (2008).
27. S. Klingebiel, I. Ahmad, C. Wandt, C. Skrobol, S. A. Trushin, Zs. Major, F. Krausz, and S. Karsch, "Experimental and theoretical investigation of timing jitter inside a stretcher-compressor setup," submitted to *Opt. Express* (2011).
28. G. Arisholm, "General numerical methods for simulating second-order nonlinear interactions in birefringent media," *J. Opt. Soc. Am. B* **14**(10), 2543–2549 (1997).
29. I. Ahmad, S. Trushin, Z. Major, C. Wandt, S. Klingebiel, T. J. Wang, V. Pervak, A. Popp, M. Siebold, F. Krausz, and S. Karsch, "Frontend light source for short-pulse pumped OPCPA system," *Appl. Phys. B* **97**(3), 529–536 (2009).
30. I. Ahmad, L. Bergé, Zs. Major, F. Krausz, S. Karsch, and S. A. Trushin, "Redshift of few-cycle infrared pulses in the filamentation regime," *New J. Phys.* **13**(9), 093005 (2011).
31. I. Ahmad, S. Klingebiel, C. Skrobol, C. Wandt, S. Trushin, Z. Major, F. Krausz, and S. Karsch, "Pump-seed synchronization measurements for high-power short-pulse pumped few-cycle OPCPA system," in *Advanced Solid-State Photonics*, OSA Technical Digest Series (CD) (Optical Society of America, 2010), paper AMB9.

32. Zs. Major, S. Klingebiel, C. Skrobol, I. Ahmad, C. Wandt, S. A. Trushin, F. Krausz, S. Karsch, and D. Dumitras, "Status of the Petawatt Field Synthesizer - pump-seed synchronization measurements," AIP Conf. Proc. **1228**, 117–122 (2010).
33. J. A. Fülöp, Zs. Major, A. Henig, S. Kruber, R. Weingartner, T. Clausnitzer, E.-B. Kley, A. Tünnermann, V. Pervak, A. Apolonski, J. Osterhoff, R. Hörlein, F. Krausz, and S. Karsch, "Short-pulse optical parametric chirped-pulse amplification for the generation of high-power few-cycle pulses," New J. Phys. **9**(12), 438 (2007).

1. Introduction

High-power, few-cycle light pulses are of great interest for studying laser-matter interactions at extreme conditions. A number of applications such as the generation of monoenergetic electron beams or the generation of intense single attosecond pulses from the solid-density plasmas has already emerged from this field [1–5] and call for light sources delivering ever shorter and more powerful pulses. Conventional laser amplification combined with the chirped pulse amplification (CPA) scheme [6], allows for achieving laser pulses with peak-power levels up to the petawatt scale by amplifying a temporally stretched pulse and subsequent compression. However, the pulse duration of the amplified pulses is limited by the laser material to a few tens of femtoseconds. Optical parametric amplification (OPA), which does not suffer from such limitations, has been identified as a promising alternative for generating high power, few-cycle light pulses. Combining the OPA technique with the CPA scheme (OPCPA) enables us to reach ultra high powers [7]. To date, the capability of OPCPA to generate PW-scale pulses on one hand [8,9] and few-cycle pulses on the other [10–12], has been demonstrated. However, it remains a challenge to reach PW-peak powers and few-cycle pulse durations simultaneously.

Since the discovery of OPA a large variety of nonlinear optical crystals have been utilized, newly introduced and engineered in order to optimize the amplification process in terms of the achievable amplification bandwidth. BBO (β -BaB₂O₄), PPLN (periodically poled LiNbO₃), LBO (LiB₃O₅) and KTP (KTiOPO₄) are most commonly used due to their high nonlinear coefficients, availability and broad gain bandwidths in the visible and NIR spectral range [7,10–19]. A sub-3 cycle, 16 TW light source, which utilizes BBO as an amplification medium, is already in operation [11]. However, these crystals are only available in limited sizes, i.e. present-day technology can provide a maximum aperture of only a few centimeters for BBO and even less for PPLN. In order to generate Joule-scale amplified pulse energies, however, crystal apertures of the order of tens of centimeters are needed to avoid optical damage and unwanted nonlinearities. Alternative crystals such as, KDP (KH₂PO₄), DKDP (KD₂PO₄) [20] and CLBO (CsLiB₆O₁₀) [21] become attractive for such systems despite their comparatively lower nonlinearity, since they can be grown in sizes of 40 cm and more in aperture. Since the gain bandwidth of DKDP exceeds that of KDP and CLBO [20,22], this has been the crystal of choice for the final amplification stages in recent high-power projects [8,9,23].

In these petawatt-class systems pulses of 100 ps – ns duration are used to pump the parametric amplifier chain. PW-scale peak powers are reached in pulses with a duration of a few-tens of femtoseconds. However, it is not possible to simply scale this scheme to the few-cycle regime while keeping Joule-scale pulse energies owing to the limited gain bandwidth in thick crystals and optical damage issues. A modified short-pulse pumped OPCPA technique which utilizes high power, few-ps pulses to amplify a broadband signal in thin OPA crystals has been suggested as a viable route towards few-cycle, Joule-scale pulses [24]. The feasibility is also supported by design calculations presented in [25]. Here, the large bandwidth is achieved by using thin OPA crystals, while the high gain and pulse energies are ensured by intense pumping and large crystal size, respectively.

The Petawatt Field Synthesizer (PFS), currently under construction at the Max-Planck-Institut für Quantenoptik (Garching, Germany), will use this short-pulse pumped OPCPA scheme to deliver fully wave-form controlled (i.e. carrier phase stabilized), few-cycle (5 fs) laser pulses with an energy of > 3 J at a repetition rate of 10 Hz. The spectral range of the PFS

pulses will be approximately 700-1300 nm, since especially for the final amplification stages thin DKDP crystals (2-5 mm) will be used in a non-collinear configuration. The special pump source required by the short-pulse pumped OPCPA scheme will deliver 1-2 ps pulses with 15-20 J total pulse energy in the green, i.e. 50 J before frequency doubling, at 10 Hz repetition rate. This pump source is currently under construction [26,27]. According to our design study these high power pump pulses will be used to amplify the μ J-scale broadband signal pulses to the desired \sim 3 J pulse energy in a chain of 7-8 OPCPA stages. The details of this design and the model of our simulations will be discussed in the following section of this paper.

Although it has been demonstrated that DKDP is suitable for the amplification of narrowband pulses to the PW-level, e.g., 43 fs in 0.56 PW [8], a detailed experimental investigation of its ability to amplify an even broader spectral bandwidth that can support few-cycle pulses, as predicted by theory, is yet to be done. We present here the first experimental findings where we have studied the amplification dynamics of OPA performed in thin DKDP crystals, pumped on the ps timescale. We have measured the broadband small-signal gain as well as the behaviour in saturation and we have compared the results with our OPA simulations. We discuss the implications of these findings in terms of the scalability of short-pulse pumped OPCPA to the PW level.

2. Theoretical modelling

We performed “pseudo 3D” modelling of the process using the Fourier split-step method [28]. The three coupled wave equations, describing the OPA process [14] are solved by a Runge-Kutta solver independently in two dimensions (time and one space coordinate). Dispersion effects as well as the spatial walk-off of both pulses due to the non-collinear geometry are taken into account. The simulation assumes plane and parallel wavefronts of the pump and the signal, which for our relatively small internal non-collinear angle of $<1^\circ$ is justified. The amplified energy is calculated under the assumption of a rotational symmetry in space, hence the term “pseudo 3D”. No higher order nonlinear or other parasitic processes are taken into account. To simulate the DKDP crystal, the Sellmeier equations described in [20] are implemented into the code.

Table 1. Parameters used for the Simulations

OPCPA stage	1	2	3	4	5	6	7	8	Σ over stages
pump energy	2 mJ	20 mJ	200 mJ	1 J	3 J	5 J	5 J	5 J	<20 J
crystal length (DKDP)	7.5 mm	7.0 mm	6.3 mm	5.5 mm	4.5 mm	3.5 mm	2.6 mm	2.2 mm	
output signal energy	0.2 mJ	2.2 mJ	22 mJ	123 mJ	452 mJ	1.05 J	1.68 J	2.34 J	2.34 J

For the PFS design studies we have numerically modelled the OPCPA stages with the design pump power of 4×5 J at 515 nm. The pump pulse and the OPCPA signal pulse duration (in FWHM) was taken to be 1.2 ps and 1 ps, respectively. Table 1 contains the parameters (pump energy and thickness of the DKDP crystals) for the subsequent OPCPA stages. The pump peak intensity for each stage was fixed to be \sim 100 GW/cm². The non-collinear type-I geometry was used with a phase-matching angle of 37.08° and an internal pump-signal angle of 0.92° . In this design study we used a different non-collinear angle than in the experiments described in this paper due to the fact that the experiments were done with a cut spectrum. These simulations were performed with the experimentally measured signal spectrum without a spectral cut. The signal spectrum and the resulting amplified spectra after each stage for the simulations are depicted in Fig. 1(a), while the extraction efficiency for each stage is presented in Fig. 1(b). It can be seen that in a series of eight amplification

stages, the signal pulses in the spectral range (730-1250 nm, measured at 10% level of maximum intensity) can reach ~2.4 J. The calculated Fourier limited pulse duration supported by the spectrum after the 8th stage is 5.6 fs, corresponding to less than two optical cycles. It is worth noting that these simulations support our simple one dimensional design which has been presented in [25]. The small differences between the simulations are due to dispersion effects, the spatial walk off between pump and signal and the spatial behaviour of the amplification process, which are not considered in the 1D code.

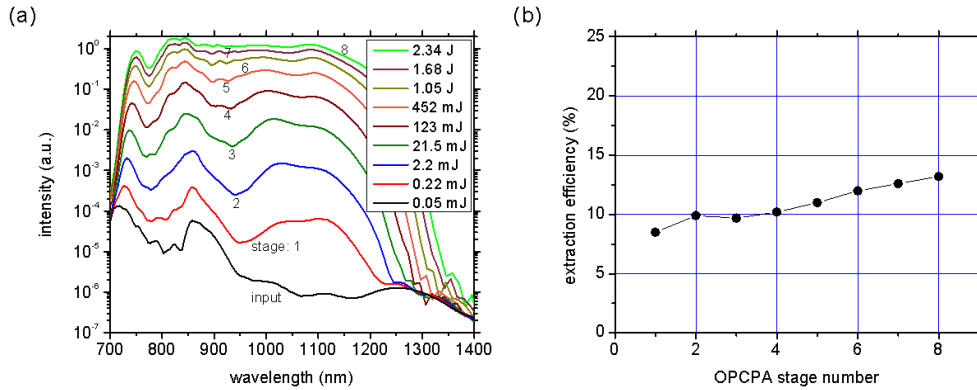


Fig. 1. (a) Calculated amplified spectra for different OPCPA stages of PFS with anticipated pump energy of 20 J. (b) Extraction efficiency $(E_{\text{signal}}^{\text{out}} - E_{\text{signal}}^{\text{in}})/E_{\text{pump}}$ of these stages.

In order to verify the validity of our “pseudo 3D” simulations we have carried out a comparison between the predictions of our model and the experiment, which are described in the next sections.

3. Methods

3.1 Experimental setup

The parametric amplification experiments were carried out using the available PFS frontend, broadband signal generation stage and first amplifier stages of the ps pump laser chain. The schematic layout of the setup is shown in Fig. 2.

The frontend laser system delivers optically synchronized seed pulses for both the pump laser chain and the OPCPA chain by deriving them from a common “master oscillator” (MO). The broadband OPCPA signal is generated by spectral broadening using a cascaded setup of Ne-filled hollow core fibers (HCF). The resulting spectrum is shown in Fig. 3. The output of the second HCF has 200 μJ of pulse energy, out of which 50 μJ are contained in the spectral range of 700-1400 nm, which is relevant for amplification in DKDP pumped at 515 nm. The frontend architecture and the spectral broadening scheme are described in full detail in [29–32]. The broadband signal pulses are temporally stretched, in order to match their duration to the pump pulses, using a prism-pair stretcher. Thus, the pulses have negative chirp in the OPCPA chain, allowing for high-throughput, simple recompression schemes, such as bulk material in combination with chirped mirrors.

Owing to the target parameters of the pump pulses (ps-scale multi-10-Joule pulses), the pump laser chain itself is a CPA system. The seed pulse for this CPA chain is derived from the master oscillator of the PFS frontend to ensure optical synchronization. Details of the seed generation for the pump laser chain are also given in [29]. The current configuration of the pump laser chain contains two subsequent Yb-doped fiber amplifiers, a grating stretcher, an Yb:glass regenerative amplifier, an Yb:YAG booster amplifier in multipass geometry and a grating compressor. The amplified pulses have a pulse energy of 300 mJ before compression within a bandwidth of ~3.5 nm, which is then temporally compressed to ~1.0 ps at a pulse energy of ~200 mJ. The details of the pump laser configuration used for the present

experiments are described in [26,27]. The compressed output is then frequency doubled in DKDP. For our first OPA experiments we used a fraction of the available pump energy and combined it with our broadband signal pulse in the DKDP OPA crystal in the non-collinear geometry to allow for the broadest bandwidth and to aid the separation of the beams after amplification.

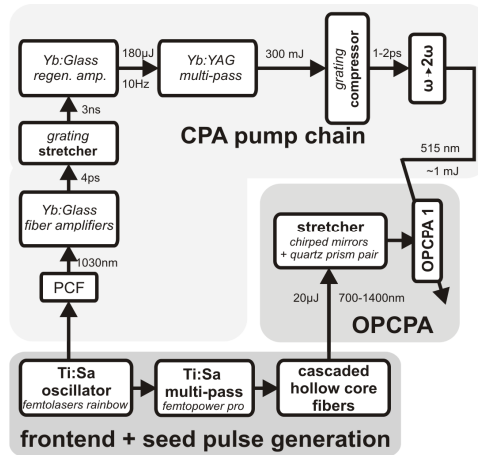


Fig. 2. Experimental setup.

3.2 OPCPA experiments in DKDP

Using the signal and pump pulses described above, we investigated the dynamics of the parametric amplification process in DKDP. For our measurements a small fraction ($\sim 800 \mu\text{J}$) of the total available pump laser energy at 515 nm is used with a FWHM duration of ~ 2 ps, i.e. slightly longer than the best achievable performance, since in this way the effect of the timing jitter can be reduced further. The pump pulse duration was adjusted by clipping the spectrum inside the grating compressor. For the amplification measurements we worked in the focus of both the pump and signal beams and thereby obtained near-Gaussian beam profiles in the OPA crystal of $1/e^2$ beam diameters of 1.3 mm and 1.2 mm, respectively. The signal beam was focused with an $f = 5$ m silver coated mirror to match the pump beam size. To focus the pump beam a slightly misaligned telescope, consisting of a focusing and defocusing lens, with an effective f -number of ~ 2000 was used. The pump intensity was limited to $\sim 100 \text{ GW}/\text{cm}^2$, which can be regarded as a safe mode of operation, since the AR coating of the DKDP crystal (515 nm and 700-1400 nm) is the limiting factor in terms of damage in the amplifier stage and its damage threshold was measured to be $\sim 300 \text{ GW}/\text{cm}^2$ in our experiment. The internal non-collinear angle between the pump and signal was fixed to 0.75° . The broadband signal spectrum after the cascaded HCF is shown in Fig. 3. It has a spike at 720 nm which is of approximately two orders of magnitude higher than the spectral intensity at 1000 nm. This peak will quickly saturate during the OPA process. Moreover it results in saturating the spectrometers and other diagnostics. Therefore in order to measure the small signal gain for the entire wavelength range correctly, we suppressed it by using a 2 mm thick RG1000 bandpass filter. The spectrum after the RG1000 filter is also shown in Fig. 3. The energy of the broadband signal after the RG1000 filter was $\sim 4.5 \mu\text{J}$.

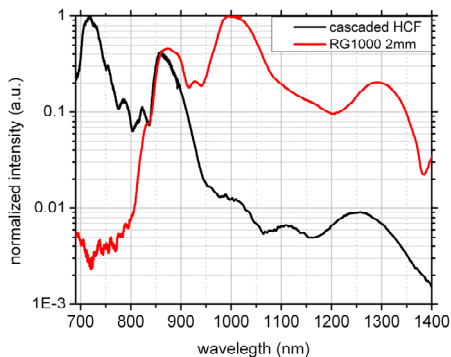


Fig. 3. Broadband OPCPA signal spectra, normalized to the peak values, at the output of cascaded hollow core fibers (black) and after a 2-mm thick bandpass filter (RG1000) shown in red.

Firstly, we investigated the small-signal gain, i.e. the regime where the amplification is far from saturation, at different phase matching angles in a 3 mm thick DKDP crystal (cf. Fig. 4). For this the signal energy was reduced to the nJ-level using a variable neutral density filter in order to avoid saturation of the OPA process. The GD between 700 and 1400 nm of the broadband signal was measured to be 700 fs. The details of the stretcher and characterization of its dispersion are described in [29]. The amplified spectra were measured using a combination of the AvaSpec-3648 and AvaSpec-NIR256-1.7 (Avantes) spectrometers in order to resolve both the visible and the near IR spectral regions.

Secondly, we measured the input signal energy dependence of the OPA gain in order to characterize the amplification behaviour in saturation. We performed this measurement using the pulse before spectral broadening and before stretching as a signal, since in the geometry of our OPA setup the pulse energy of the stretched broadband pulse ($\sim 4.5 \mu\text{J}$ after the RG1000 filter) would have been too low to achieve saturation. On the other hand the spike of the spectrum without the RG1000 filter would have saturated the OPA process very quickly for parts of the spectrum, which does not represent the real scenario and would have been difficult to model accurately for comparison. The unbroadened signal pulse had a nearly Gaussian-shaped spectrum with a FWHM of 48 nm centered at $\lambda_0 = 780 \text{ nm}$. The pulse duration at the position of the OPA crystal was measured to be 31 fs, using the GRENOUILLE (Swamp optics). The retrieved 2nd order intensity autocorrelation of the pulse by this device is shown in the inset of Fig. 5. For the amplification a 5 mm thick DKDP crystal was used, which was aligned for maximum gain, i.e. a phase matching angle of 36.86° . The signal energy was varied using the metallic filter. A high sensitivity power meter (Laser Probe Rm-6600) was used to monitor the signal energy. The amplified signal was slightly focused into a large aperture photodiode for measuring the relative gain (i.e. the ratio of the amplified to the unamplified signal energy). The amplified signal was measured at a position where it was well separated from the pump and idler beams, which were blocked by an iris, in order to minimize their contribution to the measurements.

Finally, in order to determine the extraction efficiency under saturation, for our present experimental conditions, we used a 7 mm DKDP crystal. The signal spectrum after the RG1000 spectrum was stretched in such a way to have a GD of $\sim 1.5 \text{ ps}$ for a spectral range of 800-1325 nm, by adjusting the prism separation in the stretcher as shown in Fig. 6. The phase matching angle was adjusted to have amplification in the NIR tail with its maximum at 1100 nm.

4. Results and discussion

In the following we present the results for the experiments described above. The interpretation of these findings is aided by our calculations which we used to model the scenario. In these calculations we have simulated the real scenario by taking the measured pump and signal energies, beam sizes, crystal thicknesses and non-collinear angle. The only adjustable parameter we used is the phase matching angle. Owing to the usual uncertainty in the cut-angle information provided by the crystal manufacturers, this assumption is justified.

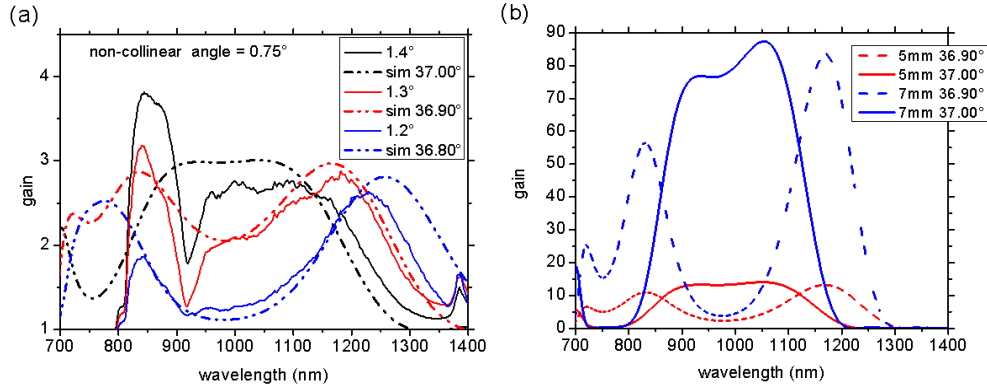


Fig. 4. Investigation of the small-signal gain: (a) Measured gain (solid lines) versus calculated gain (dotted lines) for a 3 mm thick DKDP crystal for three different phase matching angles. The crystal was cut for a phase matching angle of $\sim 37.1^\circ$, according to the manufacturer. The angles for the experimental curves are given as the deviation from the nominal cut angle. For the calculation an offset in the phase matching angle has been chosen to achieve the best possible fit with experiment. (b) Calculated gain for 5 mm and 7 mm DKDP crystals for two different phase matching angles.

4.1 Small-signal gain

The measured small-signal gain curves for different phase-matching angles are shown in Fig. 4(a). The gain curves are averaged over 100 shots to eliminate the effect of shot-to-shot instabilities. As can be seen from the measured curves, very broadband amplification was achieved with a significant gain over a bandwidth of ~ 500 nm for a phase matching angle of 37.00° . Moreover, the gain curve is very sensitive to the phase matching angle and changes its shape significantly when the phase matching angle is slightly detuned. Therefore, when working in the near field, the collimation of the beams should be better than 1 mrad. From our measurements we can see that when the phase matching angle is reduced, the amplification extends more and more into the near infrared region and has even reached 1400 nm in our experimental setup. Since the spectrum of the signal pulse has been artificially suppressed below 800 nm using a bandpass filter, no reliable gain information for this region can be extracted from our experiment. Nevertheless, our calculations predict that the gain curve extends down to 700 nm under these conditions, as shown in Fig. 4(a). In addition, a narrow dip can be observed in the measured gain curves around 920 nm. This is a combination of a very weak seed intensity in this spectral range and the way of spectral detection, since this region is situated at the edge of the sensitivity range of the visible spectrometer which therefore introduces high noise levels and delivers inaccurate measurements.

Alongside the measured small-signal gain curves, Fig. 4(a) also shows the results of our simulations of the experimental scenario, represented by the dotted lines. The calculations agree well with the measured gain curves both in absolute values and shape and the dependence on the phase matching angle is also closely reproduced. The dip in the middle of the gain curves for the phase matching angles of 36.80° and 36.90° respectively, which is due to the characteristic phase matching curve of the DKDP, is also well reproduced.

Based on the good agreement between our experimental observations and the simulations, we have performed further calculations in order to explore the parameter space for the OPA process. Since in experiments that we will discuss later, we used DKDP crystals of 5 and 7 mm thickness, we present in Fig. 4(b) the small-signal gain curves for these crystal thicknesses calculated at different phase matching angles. As expected, the gain bandwidth increases with a decrease in the crystal-thickness for optimum phase-matching conditions. It can be seen that the gain bandwidth changes from ~350 nm to ~400 nm (measured at 10% level of maximum gain) by changing crystal thicknesses from 7 mm to 5 mm for a phase matching angle of 37.00° . We can also see that although the gain bandwidth can be increased by detuning the phase matching angle, the absolute value of the gain drops.

4.2 Saturated gain measurement

As described above, we have used the 31 fs unbroadened signal pulse to investigate the amplification behaviour in saturation. We measured the output pulse energy E_{out} as a function of the input energy E_{in} and determined from this the extracted energy ($E_{\text{out}} - E_{\text{in}}$). The results are presented in Fig. 5, where it can be seen that in our setup for $E_{\text{in}} > 4 \mu\text{J}$ the OPA gain starts to be saturated. The measured temporal profile of the signal pulse is shown in the inset of Fig. 5, clearly indicating the presence of a pre/post-pulse with an intensity of approximately 10% of the main pulse. This pedestal can affect the saturation behaviour. In order to allow for a meaningful comparison between the experiment and our simulations the input pulse has to be modelled as close as possible to the experimental scenario. Since our simulation program is not able to simulate arbitrary pulse shapes in time, we performed two simulations with Gaussian pulse shape. In the first run we assumed a single 31 fs signal pulse containing all the signal energy. The calculated extracted energy for this case is marked in Fig. 5 as red circles. Owing to the fact, that this short 31 fs pulse interacts with a smaller part of the pump energy and includes a higher signal energy, we obtain a smaller extracted energy level in the simulations than we would expect from the real pulse. In our second calculation we considered two Gaussian pulses, which are amplified independently (two different simulation runs), the first one with an amplitude of 10% of the second, and the two pulses separated in time by 50 fs. We assumed, that the two signal pulses, in the simulations, see a “fresh” pump and do not affect each other. This assumption leads to an overestimation of the extracted energy. As can be seen in Fig. 5 the calculated extracted energies from this second model pulse (blue triangles) lie above the measured values. Both model calculations are consistent with the measured data. We can therefore conclude that our simulation program is able to reliably model the saturation behavior of the optical parametric amplification process.

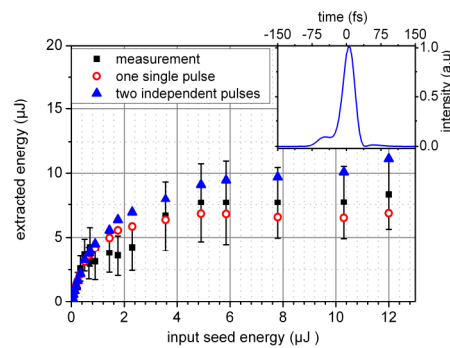


Fig. 5. Extraction energy vs. input signal energy: The black squares represent the measurements using the 31 fs input pulse (the temporal profile of which is shown in the inset). The error bars of the measured data are the standard deviation of 100 shots, which originate both from the temporal jitter and the shot-to-shot pump energy fluctuation. The red circles show the results for the calculation of one single Gaussian pulse, the blue triangles represent the results of the simulation with two independent Gaussian pulses, see details in text.

4.3 Broadband amplification

After having found good agreement in the saturation behaviour between experiment and our theoretical description in the case of the narrowband signal, we investigated the extraction efficiency in saturation using the entire broadband signal pulse. For this study we used a 7 mm DKDP crystal, which corresponds to the calculated crystal length (7.5 mm) of the first stage of the PFS system in Section 2 of this paper. The signal spectrum after the RG1000 filter was matched to the pump pulse duration in order to optimize the extraction efficiency (Fig. 6). The phase matching angle ($\sim 36.95^\circ$ from simulations) was adjusted for amplification in the NIR tail with its maximum at 1100 nm. Figure 7(a) shows the input and the amplified spectrum.

The amplification in DKDP covers the full spectrum from 830 to 1310 nm (measured at 10% level of maximum intensity). Below 800 nm no gain can be observed due to the used RG1000 filter. Even without the spectral part from 700 to 800 nm the amplified spectrum supports a Fourier limited pulse duration of ~ 6 fs which corresponds to a two-cycle pulse. To our knowledge this is the first time that such a broadband amplification in DKDP has been demonstrated. This result confirms that DKDP is appropriate for broadband amplification in ps-pumped OPCPA and supports few-cycle pulse durations.

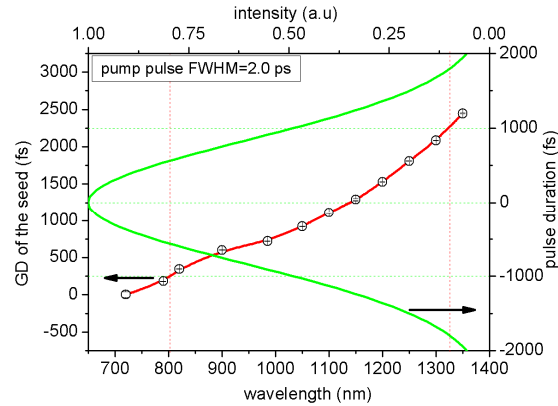


Fig. 6. Measured group delay (GD) of OPCPA signal: The NIR-tail of the signal (800-1325 nm) is stretched to fit in the FWHM duration of the pump pulse.

The broadband gain is shown in Fig. 7(b). The signal energy in the spectral range between 1100–1320 nm is much smaller compared to the energy stored in the rest of the spectrum. Therefore the amplification process is already saturated in the region around 800-1100 nm, while the spectral range between 1100 and 1320 nm experiences a gain of ~ 30 and is not saturated so far which is similar to the situation in [33]. By injection of 4.4 μJ signal energy, 53 μJ of amplified signal is obtained. This corresponds to an overall gain of 9.6 and an extraction efficiency of 6% from pump to signal.

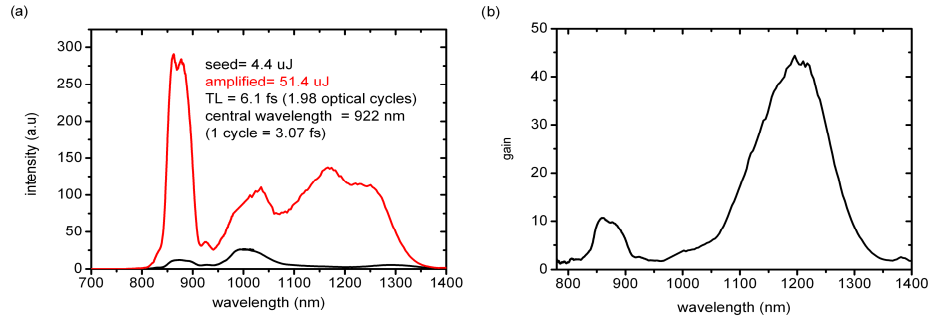


Fig. 7. (a) The amplified and unamplified spectra, using 7 mm DKDP under saturation condition. (b) Spectral gain of the amplification process extracted from (a).

5. Conclusion

We have demonstrated that the short-pulse pumped parametric amplification is feasible to deliver a sufficiently broad spectrum (cf. Fig. 7) to support a few-cycle pulse duration, with reasonable gain to reach high pulse energies up to the J level. It was shown, that DKDP crystals, which can be scaled to large apertures, pumped at 515 nm and with intensities of $\sim 100 \text{ GW/cm}^2$, are able to amplify bandwidth, supporting pulse durations of the order of ~ 6 fs. Furthermore these experiments demonstrate that the amplification bandwidth, gain and saturation agree well with that obtained from our simulations. This also justifies the validity of the Sellmeier equations [20] used in the code. Moreover this provides strong support to our design of the following OPCPA stages. However, in order to fully verify the feasibility of the PFS approach to high energy few-cycle-pulse generation it is necessary to compress the broadband amplified pulses to few-cycle duration. Measuring the phase of such broadband pulses is connected with difficulties especially for the retrieval of the higher orders in phase. In addition, the expected inherently high contrast still has to be verified experimentally using the first compressed pulses. These immediate further steps in the development of the PFS system are currently under way.

Acknowledgments

This work is funded through the PFS grant of the Max-Planck Society.